

Focused Force Transmission through an Aqueous Suspension of Granules

Bin Liu,¹ Michael Shelley,¹ and Jun Zhang^{1,2,*}

¹*Applied Mathematics Laboratory, Courant Institute of Mathematical Sciences, New York University, 251 Mercer Street, New York, New York 10012, USA*

²*Department of Physics, New York University, 4 Washington Place, New York, New York 10003, USA*
(Received 6 September 2009; revised manuscript received 7 August 2010; published 25 October 2010)

We investigate force transmission through a layer of shear-thickening fluid, here a concentrated aqueous cornstarch suspension. When a solid body is pushed through this complex fluid and approaches its containing wall, a hardened volume of the suspension is observed that adds to the leading side of the body. This volume leads to an imprint on the wall which is made of molding clay. By studying the geometry of the hardened volume, inferred by the imprint shapes, we find that its geometry is determined by the size and speed of the body. By characterizing the response of the clay to deformation we show that the force transmitted through the suspension to the wall is localized. We also study other aspects of this dynamical hardening of the suspension, such as the effect of the substrate and body shape, and its relaxation as the imposed straining is stopped.

DOI: 10.1103/PhysRevLett.105.188301

PACS numbers: 83.60.Rs, 45.70.-n, 47.57.-s

Force transmission through a medium is a fundamental subject and is crucial to many applications. A homogeneous solid subjected to an external impact or load transmits the force through elastic deformation or plastic yield [1]. In a Newtonian liquid, viscous dissipation gives rise to resistance from the straining fluid. In a granular medium, an external load causes heterogeneous force transmission, characterized by branching, chainlike structures [2–7]. Upon an external impact, both the Newtonian fluid and the dry granular medium tend to dissipate the impact force, leading to an attenuation of force intensity if measured from the other side of the medium.

We study force transmission through a *wet* granular material, here a dense aqueous suspension of microscopic cornstarch particles. It is known that such suspensions shear thicken and can show apparent divergences in shear viscosity at sufficiently high shear rates [8–11]. Extensional rheology studies likewise show divergences, and even brittle fracture at high strain rates [12]. The underlying mechanisms are not completely understood [13–16] but seem associated with the formation of particle clusters whose interactions cause jamming. In this study, we show that such a suspension can give rise to a focused force transmission. In particular, this force affects an area smaller or on the scale of the size of the moving object from which the force is initially applied. This is in contrast with other systems such as dry granular materials and viscous fluids, where an applied force becomes more dissipated and distributed through the media.

Stress propagation in dry granular media has been studied by measuring its response to the passage of a solid object [17,18]. Our experiment consists of a solid body—a plastic sphere of several millimeters in radius R —that moves through a cornstarch suspension (Fig. 1). The sphere is driven at a speed V in the range of 0.1–100 cm/s

(uniform to within 2% and with acceleration 10 m/s^2 at the start and end of each run) by a PC-controlled linear motor. It reaches any desired position with an accuracy within 0.1 mm.

We followed the protocol of Fall *et al.* [11] in preparing the suspension. Cornstarch particles (Sigma-Aldrich) are suspended at 40% by volume in a density matched mixture

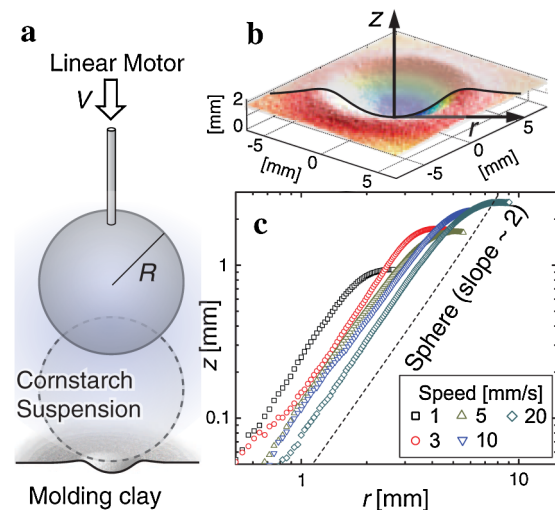


FIG. 1 (color online). A sphere, moving through a cornstarch suspension, creates a focused depression on flat molding clay. (a) The depression created by a sphere of radius $R = 12.7 \text{ mm}$ driven downward by a linear motor. The sphere stops just short of the clay surface. (b) The depression profile is digitized and shown as its elevation z against radius r . (c) Depression profiles created at different speeds V suggest hemispherical shapes. The slower the speed, the smaller and sharper the depression. The dashed line shows the corresponding profile of the sphere that caused all depressions.

of cesium chloride and water (55% CsCl by weight) [19]. Fall *et al.* studied the shear rheology of such suspensions and showed that shear thinning occurs at low shear rates with a transition to rapid shear thickening and apparent viscosity divergences at shear rates somewhat larger than unity [see Fig. 2(a) of [11]]. They interpreted this as a jamming-induced liquid to solid transition. The minimum suspension viscosity η is $O(10)$ Pa \cdot s, and so the Reynolds number $Re = \rho RV/\eta$ is between 10^{-1} and 10^{-5} , where ρ is the density of the suspension. Hence, inertial effects are negligible.

The suspension is opaque to visible light. To examine the force delivery, a piece of molding clay is prepared flat to within $50 \mu\text{m}$ and placed beneath the suspension, serving both as part of the container and as force recorder [20,21]. Each experimental run starts with the sphere fully immersed in the suspension, allowing a travel of about 4 cm in the 6 cm deep suspension before the sphere stops near, but never touching, the clay surface. As the sphere approaches the bottom, the force transmitted through the suspension deforms the clay surface once the yield stress of the molding clay has been exceeded. In a separate calibration, we determined the yield stress of the clay to be approximately 170 kPa [see Fig. 4(a)]. The resistive force upon the sphere is also monitored by a strain gauge attached between the sphere and the linear motor. The experiment is repeated while varying sphere size R , moving speed V , and halting height H above the surface. After each run, the clay is removed and its surface morphology digitally reconstructed [22].

If the sphere is halted just above the bottom, near $H = 0$, a depression is created in the clay surface (Fig. 1). This depression is smooth and hemispheric, and has a radius smaller than that of the sphere. We were unable to produce

such a feature using a Newtonian fluid, at least in the low Reynolds number regime, regardless of its viscosity. This feature is also different from those produced by force chains in a dry granular material, which would give rise to distributed, spiky indentations over a broad area [2,6,7]. Note that to have exceeded the clay yield stress for a typical case considered ($V = 2$ mm/s, $R = 6.4$ mm, giving $H \sim 1$ mm and thus a typical strain rate $V/H \sim 2$ s $^{-1}$) would require a viscosity an order of magnitude bigger than the largest value measured by Fall *et al.* in the rapid shear-thickening regime.

The shape of the depression, its depth h , and curvature κ are reproducible, given V and R . The depressions have near radial symmetry, with their contour lines at a given elevation z (measured from the bottom) being within 15% of perfect circles. We quantify the geometry of the depression in Fig. 1. It shows, for $R = 12.7$ mm, the elevation z against the radius r (averaged over experimental runs) in a log-log plot, suggesting a parabolic geometry near the bottom and an overall hemispherical depression. Each curve shown in this figure was produced with a halting height just above $H = 0$, so that the sphere never directly touches the clay surface. A fit between elevation and radius, $z = \kappa r^2/2$, yields the depression curvature κ . A large κ corresponds to a small, sharp depression. For instance, as shown in Fig. 1, the curvature and depth of the depression increase and decrease, respectively, with decreasing approach speed. Hence, lower approach speed produces more focused depressions.

By stopping the sphere at successively reduced heights H , and then digitizing the consequent depression, we can reconstruct the process of temporal progress of the depression. This interpretation relies upon the lack of inertia in the system and the plastic response of the clay, so that the depression stops developing immediately upon cessation of sphere motion. This reconstruction shows that a smooth depression on the clay develops once the sphere comes to within a distance h_0 . For a given speed, once the depression starts to develop, the gap between the bottom of the solid sphere and the bottom of the depression tends to be maintained at h_0 , namely, $H + h = h_0$ [Fig. 2(a)]. Moreover, Fig. 2(b) suggests that as the depression deepens, its curvature near the bottom tends to saturate. These two observations lead us to conclude that there exists an effective “solid” or hardened volume, which precedes the solid sphere as it approaches the wall and which maintains a hemispherical shape.

The deformation onset distance h_0 is speed dependent, increasing with increasing approach speed. This is different from the dry granule case, where the length scale at which a moving body interacts with an approaching wall is speed independent [17,18].

By the time the sphere stops at $H = 0$, the hardened suspension has “cast” itself a depression into the clay. By plotting the relative curvature κR and the scaled depression depth h/R against the strain rate $\dot{\gamma} = V/R$, we observe at higher strain rates ($\dot{\gamma} \gtrsim 0.2$) a collapse of the data (Fig. 3).

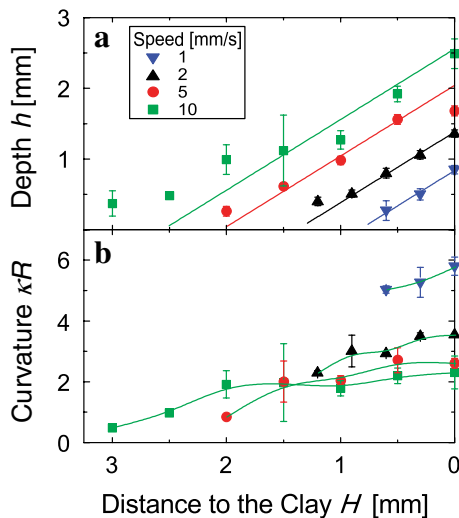


FIG. 2 (color online). The depressions in the clay resulting from a sphere ($R = 12.7$ mm) moving at various speeds V and stopping at heights H . (a) The dependence of depression depth h on H . (b) The dependence of the normalized depression curvature κR as a function of H .

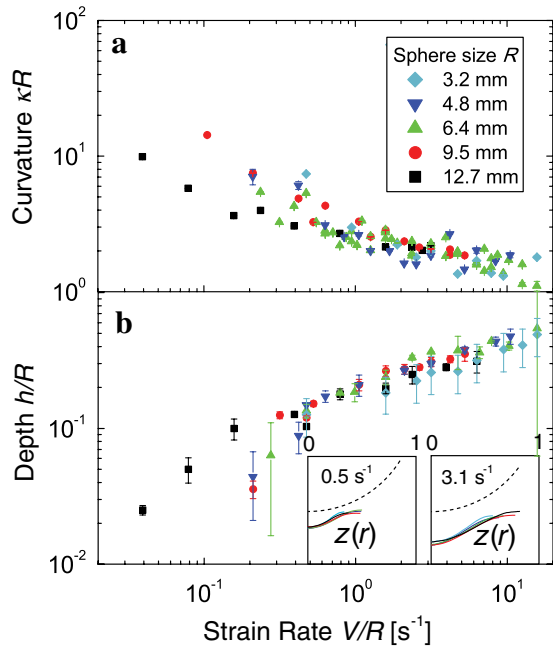


FIG. 3 (color online). The dimensionless curvature κR (a) and the dimensionless depth h/R (b) of the depression, which describe the shape of the hardened volume, plotted as a function of the characteristic strain rate $\dot{\gamma} = V/R$. The insets show two groups of depression profiles, rescaled by the radius of sphere R , at two strain rates $\dot{\gamma} = V/R = 0.5$ and $3.1 s^{-1}$, respectively. These profiles (five solid curves in each group) collapse for fixed $\dot{\gamma}$. For comparison, the rescaled sphere with radius 1 is also shown.

This suggests that the hardened suspension assumes a universal set of shapes parametrized by $\dot{\gamma}$. Hence, lower strain rates yield localized depressions of large relative curvature, and increasing strain rate yields depressions whose size and depth approach the scale of the sphere. If the system were controlled solely by the strain rate $\dot{\gamma} = V/R$, then below some critical $\dot{\gamma}$ the suspension would not be sufficiently strained to yield hardening [11,12]. In that case the extensional flow between the body and the wall, with characteristic strain rate V/H , should eventually become strong enough to yield hardening. It may be this feature that explains the lack of collapse at small $\dot{\gamma}$.

In interacting with the sphere the clay wall develops a permanent, plastic deformation. The transmitted force F_T being applied by the hardened volume is estimated by multiplying the depression area by the deformation stress of the clay [see Fig. 4(a)]. Figure 4(b) shows the estimated F_T plotted against the total resistive force F_R acting upon the sphere as measured by the attached strain gauge. While these two independent measurements are gratifyingly similar in scale, the more important feature is that the transmitted force (omitting one outlier) comprises a large proportion, 75%–95%, of the total force resisting sphere motion. Hence, we refer to the hardened volume as applying a “focused force.”

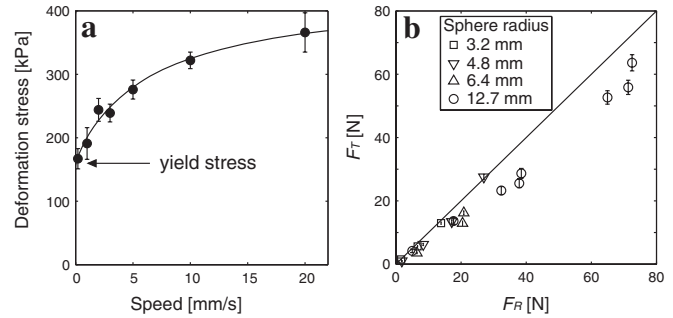


FIG. 4. (a) Calibrating the clay as force recorder. In the absence of an intervening suspension, the clay exerts a speed-dependent resistive force upon a hemispherical intruder that scales with near linearity on the deformation area. The slope gives the deformation stress $S(V)$ plotted in (a) as a function of speed V . (b) For a sphere moving with speed V through the cornstarch suspension, the transmitted force $F_T = S(V)A$, where A is the resulting depression area, plotted against the resistive force F_R .

Replacing the clay with an elastic material that can relax back to its undeformed shape allows us to investigate dynamical aspects of the suspension hardening. We now replace the molding clay with a cured polydimethylsiloxane (PDMS) substrate (10 mm thick). The PDMS is elastic, with a shear modulus on the order of 250 kPa [23]. An advantage of PDMS is its transparency, which allows visualization of its deformation. An example is shown in Fig. 5(a). The sphere approaches the PDMS wall and stops at time $t = 0$ at the height of the (original) surface. As the

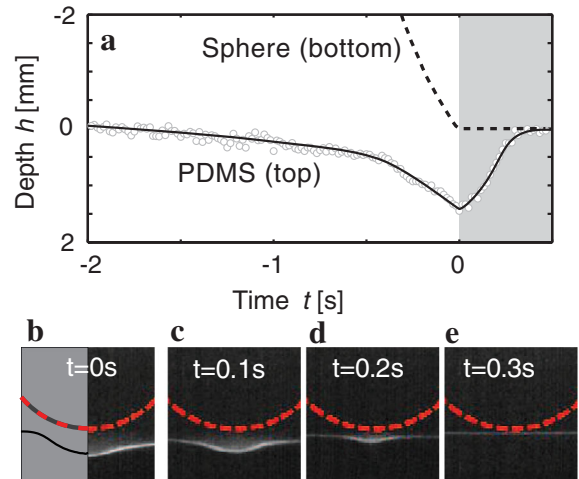


FIG. 5 (color online). Recovery of a depression on an elastic PDMS substrate. (a) The height of the PDMS surface (open circles) evolves after the sphere stops at $t = 0$ at the original height of the surface. The dashed line shows the trajectory of the sphere. Panels (b)–(e) show side views of the PDMS surface after the sphere stops moving. The position of the sphere is superimposed as the dashed curves. A depression made in clay, under the same conditions, is shown on the left side of (b), and has a profile similar to the PDMS depression.

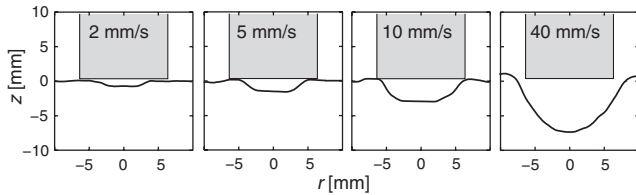


FIG. 6. A circular cylinder of diameter 12.7 mm approaches and stops near the surface of a clay substrate. The curves show the profiles of the resulting depressions left in the clay.

sphere approaches, the PDMS surface is depressed (shown by the solid curve) following the motion of the sphere (shown by the dashed curve). Though different from the clay, the depression on the PDMS has similar size and curvature [5(b)]. After $t = 0$ [shaded in Fig. 5(a)], the PDMS surface starts to relax while the sphere stays put. As the PDMS moves back to its original position it essentially maintains the depression curvature [5(b)–5(e)]. The results suggest that the hardened volume between the sphere and surface has softened and been pushed out in about 0.3 s. It should be noted that the PDMS substrate can recover much more quickly in the absence of the suspension, on about a 1 ms time scale.

We found that the onset distances h_0 were practically identical for both PDMS, clay, and for the bare, rigidly backed Plexiglass wall of the container. This comparison among substrates was done by measuring the force needed to drive the sphere at constant velocity. The force rose rapidly once the sphere was within the onset distance, with the increase being on the order of 10^3 times.

Our results argue that the motion of a body through a shear-thickening suspension leads to its local hardening. The hardened volume can be used to transmit a focused force, and we speculate that it results from a jamming of particles within the suspension [24] which is possibly amplified by the presence of walls. The hardened volume has a well-defined geometry that no doubt depends upon both the shape of the moving body and the material straining that develops around it. To demonstrate this, Fig. 6 shows the depressions that develop as a rigid circular cylinder approaches a clay substrate at various speeds. Relative to a spherical body, the depressions are deeper relative to body diameter and become hemispherical only at higher speeds. As the shape of the hardened volume is determined by and modifies the material stress distribution, this constitutes a nonlinear free-boundary problem for its shape. We are now pursuing this aspect theoretically. We also find that the hardened volume relaxes or “melts” with cessation of external driving. This jamming phenomenon is different from that occurring within dry granular materials, which can show extremely long relaxation times [25–27] given a finite material strain [28].

We are thankful for helpful discussions with P. Chaikin, T. Majmudar, and A. Weathers. This work was supported

by NSF (DMS-0652775, MRI-0821520, and DMR-0820341) and DOE (DE-FG02-88ER25053).

*jun@cims.nyu.edu

- [1] K. L. Johnson, *Contact Mechanics* (Cambridge University Press, Cambridge, England, 1985).
- [2] C.-H. Liu *et al.*, *Science* **269**, 513 (1995).
- [3] D. M. Mueth, H. M. Jaeger, and S. R. Nagel, *Phys. Rev. E* **57**, 3164 (1998).
- [4] J. S. Uehara, M. A. Ambroso, R. P. Ojha, and D. J. Durian, *Phys. Rev. Lett.* **90**, 194301 (2003).
- [5] A. M. Walsh, K. E. Holloway, P. Habdas, and J. R. de Bruyn, *Phys. Rev. Lett.* **91**, 104301 (2003).
- [6] K. E. Daniels, J. E. Coppock, and R. P. Behringer, *Chaos* **14**, S4 (2004).
- [7] M. P. Ciamarra *et al.*, *Phys. Rev. Lett.* **92**, 194301 (2004).
- [8] R. L. Hoffman, *J. Rheol.* **16**, 155 (1972); *J. Colloid Interface Sci.* **46**, 491 (1974); *Adv. Colloid Interface Sci.* **17**, 161 (1982).
- [9] E. Bertrand, J. Bibette, and V. Schmitt, *Phys. Rev. E* **66**, 060401(R) (2002).
- [10] D. Lootens, H. van Damme, Y. Hémar, and P. Hébraud, *Phys. Rev. Lett.* **95**, 268302 (2005).
- [11] A. Fall, N. Huang, F. Bertrand, G. Ovarlez, and D. Bonn, *Phys. Rev. Lett.* **100**, 018301 (2008).
- [12] E. B. White, M. Chellamuthu, and J. P. Rothstein, *Rheol. Acta* **49**, 119 (2010).
- [13] N. J. Wagner and J. F. Brady, *Phys. Today* **62**, No. 10, 27 (2009).
- [14] J. R. Melrose, J. H. van Vliet, and R. C. Ball, *Phys. Rev. Lett.* **77**, 4660 (1996).
- [15] M. Sellitto and J. Kurchan, *Phys. Rev. Lett.* **95**, 236001 (2005).
- [16] D. S. Grebenkov, M. P. Ciamarra, M. Nicodemi, and A. Coniglio, *Phys. Rev. Lett.* **100**, 078001 (2008).
- [17] M. B. Stone *et al.*, *Nature (London)* **427**, 503 (2004); *Phys. Rev. E* **70**, 041301 (2004).
- [18] Z. Peng, X. Xu, K. Lu, and M. Hou, *Phys. Rev. E* **80**, 021301 (2009).
- [19] F. S. Merkt, R. D. Deegan, D. I. Goldman, E. C. Rericha, and H. L. Swinney, *Phys. Rev. Lett.* **92**, 184501 (2004).
- [20] R. M. Schmidt and K. R. Housen, *Int. J. Impact Eng.* **5**, 543 (1987).
- [21] Y. S. Lee, E. D. Wetzel, and N. J. Wagner, *J. Mater. Sci.* **38**, 2825 (2003).
- [22] D. L. Blair and A. Kudrolli, *Phys. Rev. Lett.* **94**, 166107 (2005).
- [23] J. C. Lötters, W. Olthuis, P. H. Veltink, and P. Bergveld, *J. Micromech. Microeng.* **7**, 145 (1997).
- [24] E. Brown and H. M. Jaeger, *Phys. Rev. Lett.* **103**, 086001 (2009).
- [25] A. J. Liu and S. R. Nagel, *Nature (London)* **396**, 21 (1998).
- [26] C. S. O’Hern, L. E. Silbert, A. J. Liu, and S. R. Nagel, *Phys. Rev. E* **68**, 011306 (2003).
- [27] A. D. Gopal and D. J. Durian, *Phys. Rev. Lett.* **75**, 2610 (1995).
- [28] C. Heussinger and J.-L. Barrat, *Phys. Rev. Lett.* **102**, 218303 (2009).